



# Investigation of the Phase Mechanism Behaviors of Fe-Cr-Ni alloy by Molecular Dynamics Simulation

Merve DUMAN<sup>1</sup> , Fatih Ahmet CELIK<sup>2,\*</sup> 

<sup>1</sup>Bitlis Eren University, Graduate Education Institute, 13000, Bitlis, Türkiye

<sup>2</sup>Bitlis Eren University, Faculty of Arts&Sciences, Physics Department, 13000, Bitlis, Türkiye

## Highlights

- This paper focuses on modeling of the Fe-Cr-Ni alloys by molecular dynamics simulation.
- We examine the phase mechanism of the Fe-Cr-Ni medium entropy alloy.
- The simulation results have been compared with available experimental data in the literature.

## Article Info

Received: 16 May 2023

Accepted: 07 Dec 2023

## Keywords

Fe-Cr-Ni  
Medium-entropy alloys  
Modelling  
Molecular dynamics

## Abstract

In the presented study, Fe-Cr-Ni ternary alloy system, which is classified as medium entropy alloys, was modelled using molecular dynamics (MD) simulation method. Model system was built at specific concentration ratios in accordance with the crystal lattice structures in the phase diagrams. The potential energy function based on the Grujicic-Zhou (GZ) type embedded atom method (EAM) was chosen as the potential function suitable for the system. The phase transformation mechanisms of the model system were investigated by applying heating-cooling processes on the most stable structures. In these processes, thermodynamic parameters such as temperature, volume, potential energy and density were calculated. In addition, the phase transformation mechanism and structural properties were analysed using radial distribution functions (RDF). Three-dimensional pictures of MD cells and the number of crystal structures were obtained using the visualization and analysis software via the atomic positions obtained during the transformations. In all these processes, the results obtained by the MD calculation method were interpreted and compared with the experimental data.

## 1. INTRODUCTION

Nanotechnology applications are widely used in producing metallic alloys, classified according to their components or concentration [1–3]. In this classification, high entropy alloys differ from traditional alloys, as at least five elements come together and introduce secondary properties with a concentration ratio ranging from 5 to 35 percent. This main characteristic affects some of the physical properties of the alloys, such as hardness, corrosion resistance, high wear, and oxidation resistance [4, 5].

In recent years, the use area of medium entropy alloys has constantly increased due to their better mechanical properties than high entropy alloys [6]. Among these alloys, Fe-Cr-Ni medium entropy alloys, which have attracted considerable attention, have been found to have advantageous properties such as high strength, corrosion resistance, low thermal expansion coefficient, and coating properties [7, 8]. Therefore, many experimental studies have been conducted on this alloy to understand some of its complex properties [9, 10]. Among the studies performed on Fe-Cr-Ni medium entropy alloys, the study conducted by Blinova et al. investigated the effect of large plastic deformation and austenitic-martensitic transformation induced in Bridgman anvils on their mechanical properties in microstructure [11]. Furthermore, Mahesh et al. studied whether or not bimodal grain size distribution, rather than nano-crystalline grain size, can significantly improve the ductility of these alloys [12]. Du et al. made a comparative analysis on the oxidation behavior of Ce-containing Fe–Cr–Ni medium alloy in the temperature range of 950~1050 °C in

\*Corresponding author, e-mail: facelik@beu.edu.tr

a certain period of time [13]. Zhang et al. examined the precipitation behavior of Ni<sub>3</sub>(Ti, Al) and the bulk mechanical properties using Fe–Cr–Ni maraging stainless steel [14].

These studies revealed that some properties of Fe-Cr-Ni alloy have not yet been explained because of experimental deficiencies. However, upon the development of various computational methods, it has become possible to obtain incomplete and unavailable analyses due to the difficulties associated with experimental conditions [15]. This is especially relevant, as performing some experiments is extremely difficult or economically challenging. However, computational methods offer researchers many advantages in terms of cost, time, and safety [15, 16]. The most important one of these methods is molecular dynamics (MD) computer simulation, which has recently become an important tool in scientific studies to compare the predictions of theoretical models with experimental results [16]. In an MD method, the position and velocity of atoms and molecules placed in a computational box or cell are calculated in phase space using the laws of Newton's equations of motion. In general, the initial velocities of the atoms, the positions where the atoms must be placed according to the structure of the lattice to be built, and the environmental conditions are determined in the initial stage [17]. Subsequently, the forces acting on each atom are calculated using a potential energy function to represent the interatomic interactions. In the next step, some numerical integration algorithms are used to predict where the atoms will be placed in phase space in the subsequent step. In the final step, a series of measurements are made on the model system in equilibrium to obtain thermodynamic, dynamic, and structural properties [18, 19].

An extensive literature review reveals that few MD simulation studies are conducted on Fe-Cr-Ni medium entropy alloys. Among these studies, the research conducted by Mahata et al. investigated the mechanical properties of nanowires composed of Fe-Cr-Ni alloy through MD using the EAM and first principles approach [20]. Wu et al. developed a modified EAM (MEAM) potential for the Fe-Cr-Ni ternary system based on previously developed MEAM potentials for pure Cr, Fe, and Ni [21]. In addition, Li-Juan You et al. discussed the effect of Cu precipitation on tensile properties of Fe–Cu–Ni alloy via MD simulation [22]. Das et al. worked the surface morphology of Fe–Cr–Ni ternary alloys with stress corrosion cracking mechanism by quantum chemical MD approach [23]. Wang et al. studied the interfacial phase stability and grain boundary phase diagrams in Fe-Cr-base alloy systems as Fe-Cr-Ni [24]. Kumar et al. have used large-scale MD simulations to investigate the evolution of variety of crystal-type structures in Fe–Cr–Ni alloy during solidification [25].

In this study, Fe-Cr-Ni medium entropy alloy was modeled using MD method. Grujicic-Zhou (GZ) type potential energy function based on the EAM was used for interactions between atoms. Based on the experimentally known phase diagrams of model system, heating-cooling and rapid cooling from the liquid phase were performed and the structural transformations of the phase regions were compared. In all these processes, the thermodynamic parameters of the model system were obtained. Also, the characteristics of the structural transformations are analyzed using radial distribution functions

## 2. MATERIAL METHOD

### 2.1. Potential Energy Function

The dynamical processes of model system, it is necessary to use their motion and velocity at the molecular scale, and therefore with embedded atom method (EAM), which predicts an approximate calculation of the various interatomic forces which are determined from the potential energy of the system [26]. EAM was often chosen along the lines of effective-medium theory represented as a collection of effective atom [27]. In this representation the average energy per atom,

$$\langle E \rangle = \frac{1}{N} \left[ \sum_{i=1}^N F_i(\rho_i(\mathbf{r}_i)) + \frac{1}{2} \sum_{\substack{i,j=1 \\ i \neq j}}^N \Phi(r_{ij}) \right] = \langle F_i(\rho) \rangle = \frac{1}{2} \langle \sum_{\substack{j=1 \\ (j \neq i)}}^N \Phi(r_{ij}) \rangle \quad (1)$$

where  $\rho_i$  (electron density) is assumed to be fairly uniform from atom to atom. An average atom is can be rewritten by interaction with a Ni atom [27]

$$\phi_{Ni-n}(r) = X_{Ni}\phi_{Ni-Ni}(r) + X_M\phi_{M-n}(r) = \frac{Z_{Ni}(r)}{r} [X_{Ni}Z_{Ni}(r) + X_MZ_M(r)] = \frac{Z_{Ni}(r)}{r} \langle Z(r) \rangle . \quad (2)$$

## 2.2. Simulation Details

In the simulation studies, the phase transformation processes of the Fe-Cr-Ni alloy at different temperatures were performed using Scigress commercial source software code [28]. The Grujicic-Zhou based EAM potential energy function (PEF) proposed by Smith et al., was used for the Fe-Cr-Ni model system [27]. To determine the reliability of the PEF, the model system was equilibrated in phase space. For the Fe-Cr-Ni ternary alloy system, 3000 atoms of nickel, 750 atoms of Fe and 250 atoms of Cr were used for a total of 4000 atoms. The MD computational cell was created by applying periodic boundary conditions in three dimensions to the model system. The Maxwell velocity distribution appropriate for the desired temperature was used to determine the initial atomic velocities. The unit MD step was set to 1.0 fs and the 5th order predictor-corrector Gear algorithm was chosen for the integration step size. The NVT canonical statistical ensemble was used to describe the thermodynamic states of the model system. In all simulations, the velocities of the atoms in the MD cell were scaled and the Nose-Hoover thermostat algorithm was preferred for temperature control [29]. The temperature of the model system was heated starting from 300 K to 1200 K and kept at these temperatures for a total of 30 ps during the heating process. Also, the temperature of the model system was raised to 3000 K within 10 ps, held at this temperature for 10 ps, and cooled again within 10 ps by decreasing of temperature to 300 K with a high cooling rate of  $10^{14}$  K/s.

## 2.3. Radial Distribution Functions (RDF)

The structural changes determined by the arrangement of atoms during phase transformations can be determined by the RDF. This function analyzes the probability of atoms remaining in a circle (volume element) of thickness  $\Delta r$  and radius  $r$ , located at a distance  $r + dr$  from the central atom (or an atom chosen as a reference). In this case,  $n(r)$  is the number of atoms remaining in this volume (V) element. RDF is defined as follows [30]:

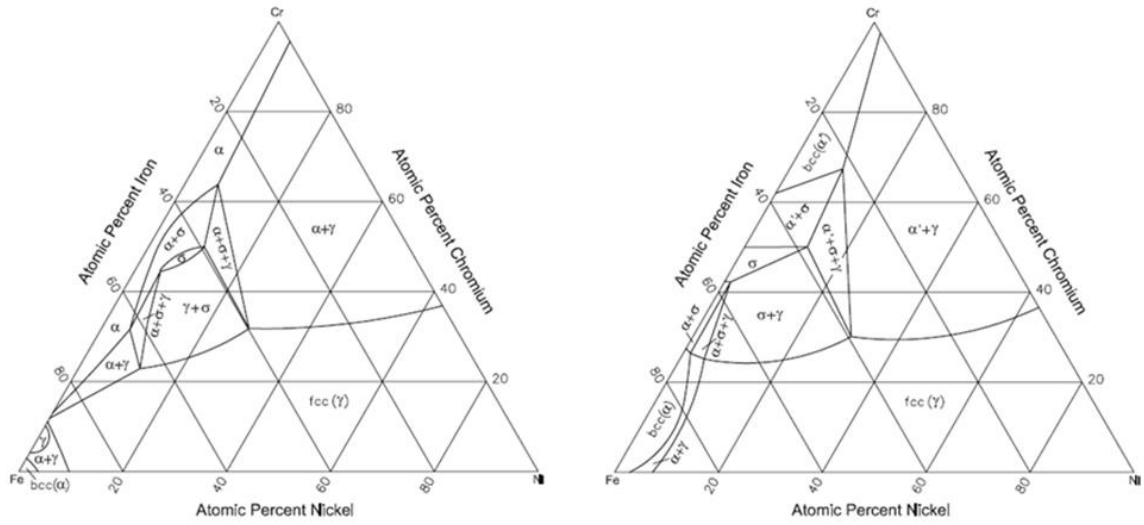
$$g(r) = \frac{V}{N^2} \left\langle \sum_{i=1}^n \frac{n(r)}{4\pi r^2 \Delta r} \right\rangle \quad (3)$$

In a periodic crystal structure with long-distance arrangement, the heights of the peaks corresponding to the atomic distances are high and sharp. In liquid and amorphous structures, which do not exhibit long-distance arrangement, the atomic distributions are more irregular, so there is a higher peak at the nearest adjacent distance, indicating a high probability of atoms in the nearest adjacency. Subsequent peaks decrease in intensity with increasing  $r$  atomic distances and as a result, the average intensity becomes stable at a point [17, 30].

## 3. THE RESEARCH FINDINGS AND DISCUSSION

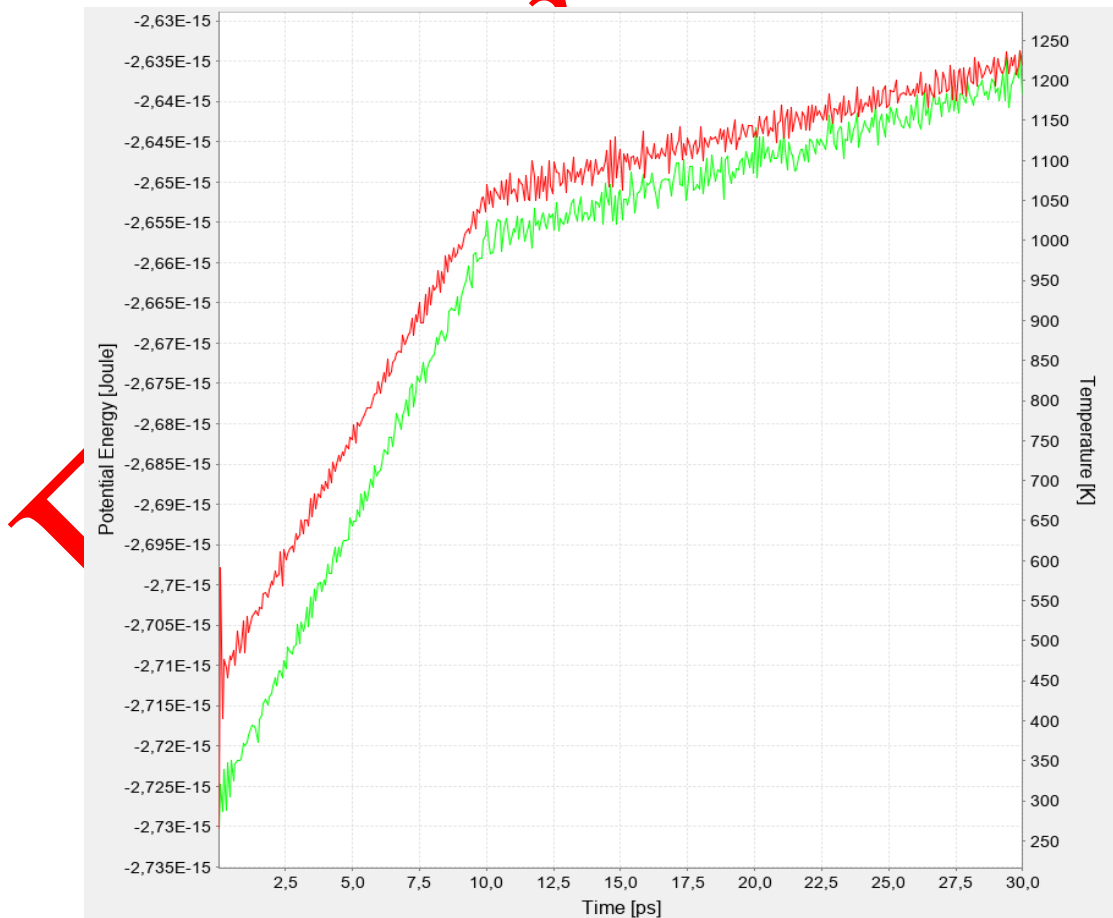
### 3.1. Phase Mechanism of Model System

Figure 1 shows the experimentally determined phase diagram for the Fe-Cr-Ni ternary alloy [31]. Upon examining the phase diagram, it was observed that the face-centered cubic (FCC) ( $\gamma$ ) phase did not change between 750°C and 850°C for the region with high concentrations of Ni atoms and low concentrations (atomic percentage) of Fe and Cr atoms. More mixed-phase transformations occurred as the Fe concentration increased.



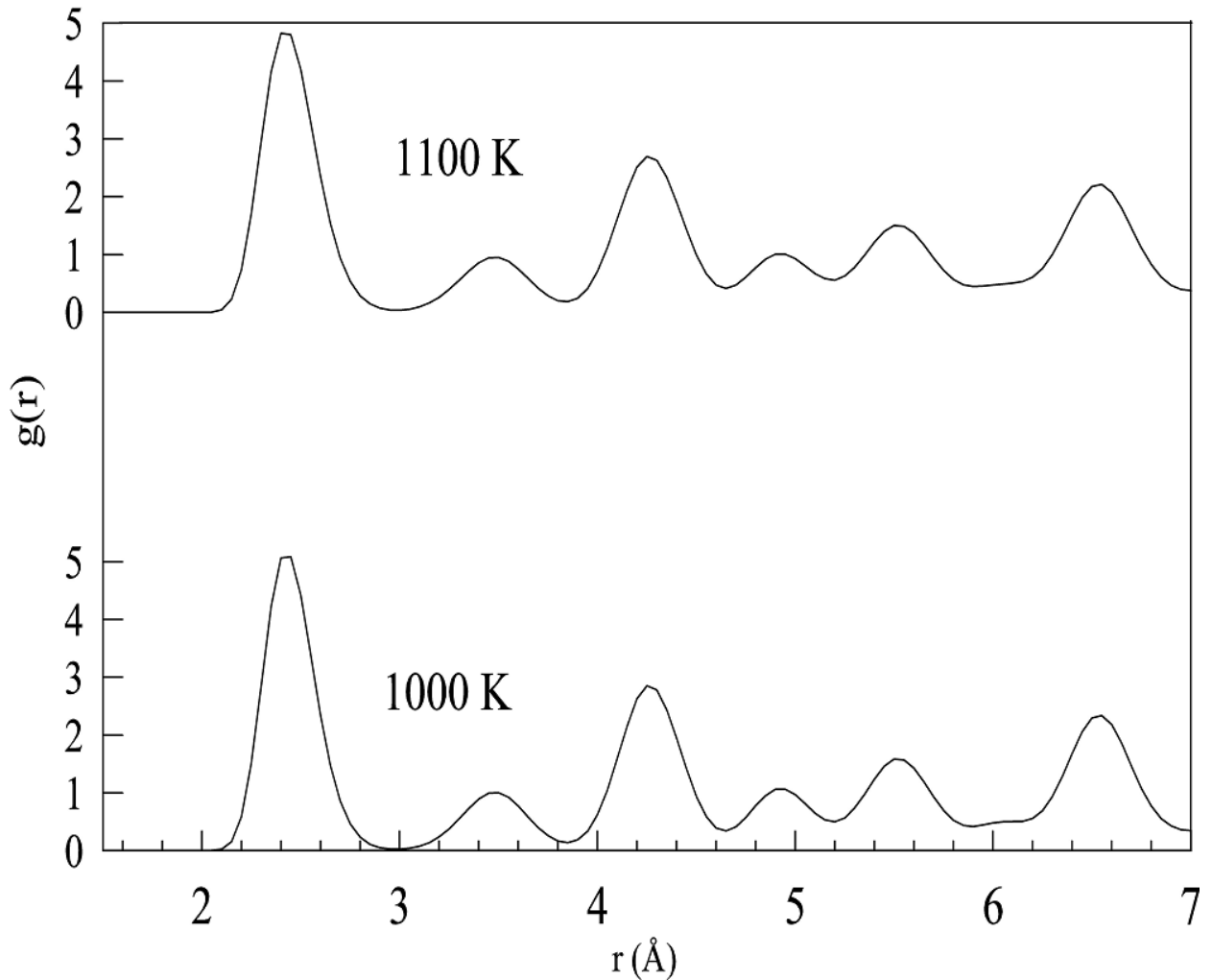
**Figure 1.** The phase diagram of Fe-Cr-Ni at 750 and 850 °C [31]

Figure 2 shows the model system's potential and temperature variation with simulation time. The system's temperature was increased from 300 K to 1000 K in 10 ps. Subsequently, the temperature was increased from 1000 K to 1200 K in 20 ps time. The energy increased as the temperature increased in the heating process. This increment can be interpreted as an increase in the system's atomic vibrations and mobility. Therefore, the atomic rearrangements occur with increasing temperature during the heating process.



**Figure 2.** Potential energy and temperature change in the heating process of the model system

The RDF analysis describes any system's atomic arrangements and structural interactions [32]. The first peak of the RDF or  $g(r)$  is proportional to the number of nearest neighbors, and the loss of sharpness of the peaks means that phase transformations occur with the increase of atomic vibrations [33]. Figure 3 shows the total RDF curves obtained at 1000 K and 1100 K during the heating process of the system. The figure shows that the RDF curves represent the ideal FCC structure at 1000 K and 1100 K temperatures. It means that no phase transformation occurred in this temperature range. This result is consistent with the experimentally obtained phase diagram of the system in Figure 1.



**Figure 3.** The RDF curves obtained at certain temperatures during the heating process for the model system

Figures 4 and 5 show the MD cells formed by the atomic positions obtained at 1000 K and 1100 K for the Fe-Cr-Ni system. It was observed that the atomic distributions and planes forming the MD cells were ordered with the same periodicity. At 1000 K and 1100 K, it can be concluded that the crystal structure of the system did not change. This result is consistent with the experimentally obtained phase diagram and RDF curves of the alloy system [where orange colors represent iron (Fe), and yellow and blue colors represent nickel (Ni) and chromium (Cr) atoms, respectively]

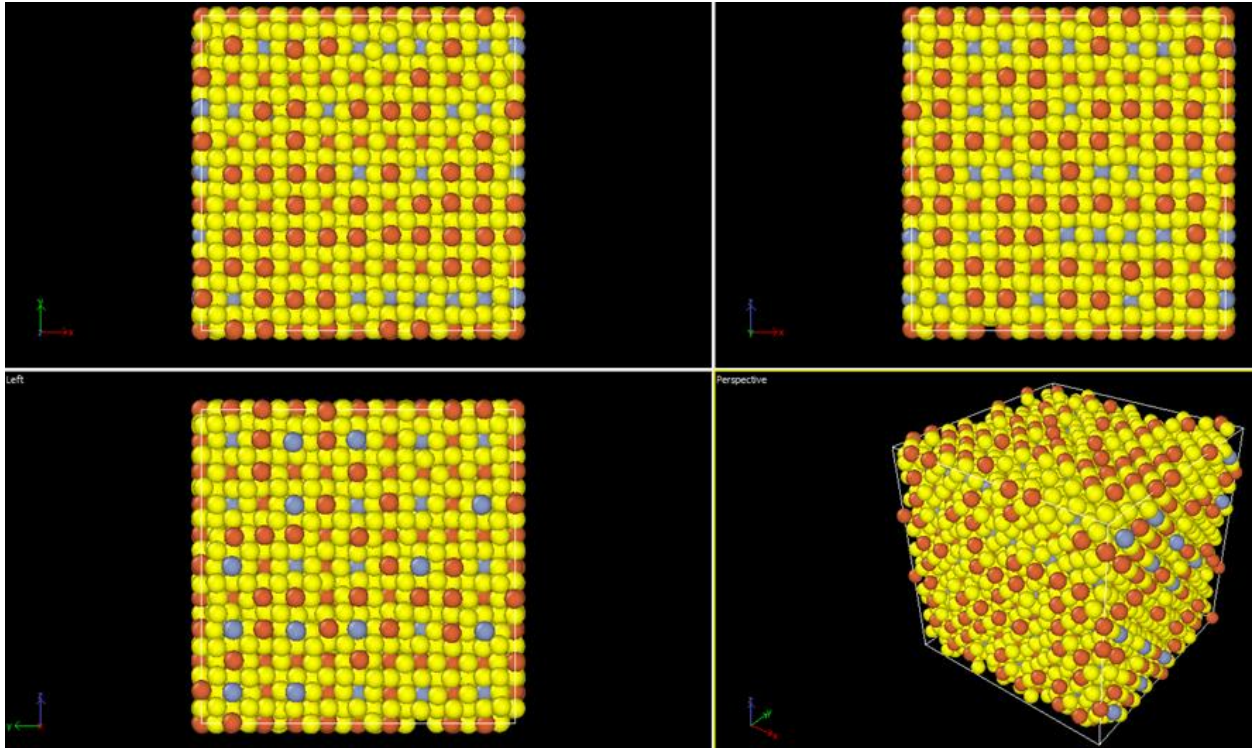


*Figure 4. Atomic distribution image in the MD cell at 1000 K for the model system*

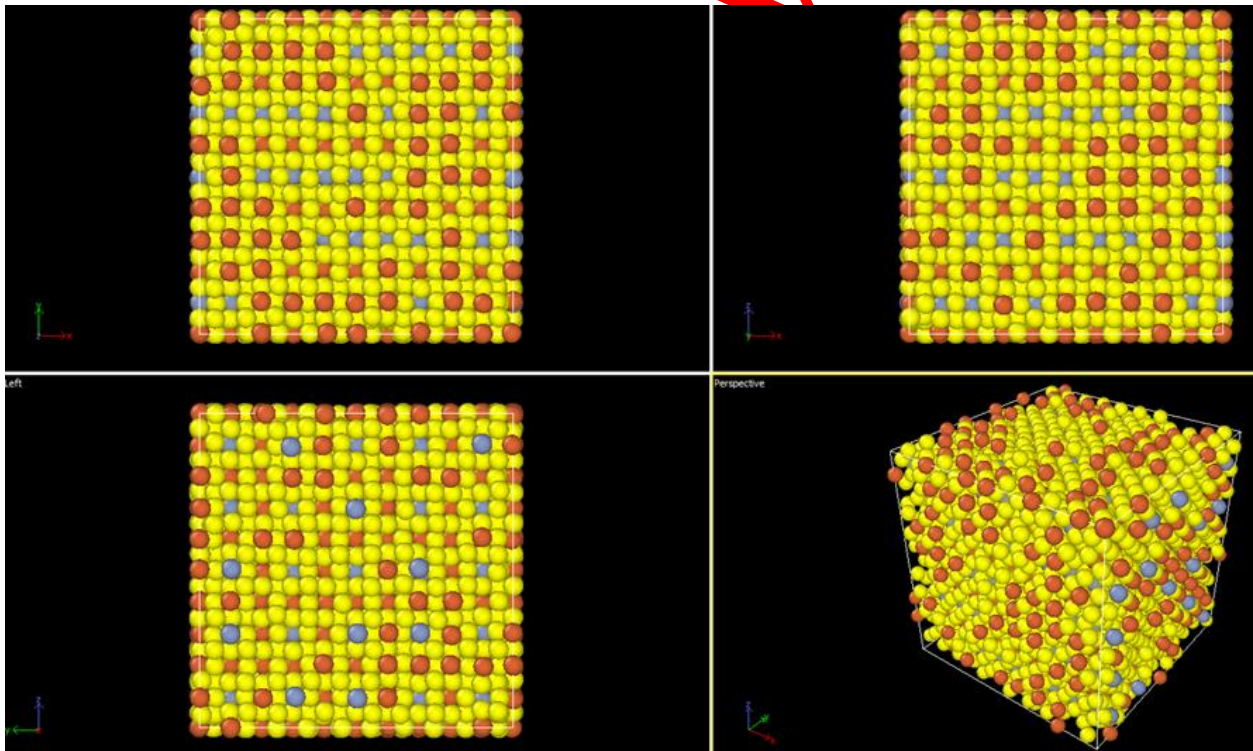


*Figure 5. Atomic distribution image in the MD cell at 1100 K for the model system*

The percentage numbers of crystal-type lattice structures in the system can be examined using the OVITO visualization and structural analysis program [34]. Figure 6 shows the percentage values and the image of the MD cell obtained at 1000 K and 1100 K of different crystal systems obtained using the OVITO program. When the percentages of the crystal structures comprising the system were examined, FCC crystal lattices were dominant in a large proportion (~99.5 percent) at both temperatures.

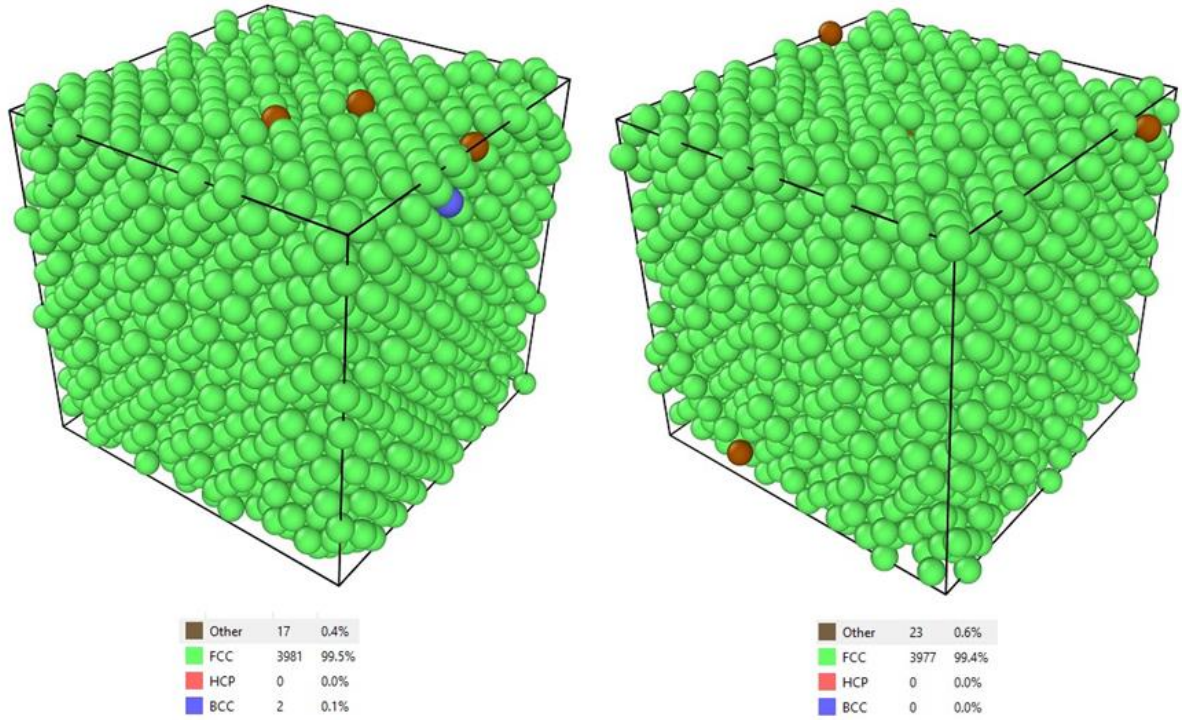


**Figure 6.** Percentage ratios of crystal lattice and other structures obtained at 1000 K and 1100 K temperatures of the model system (FCC: face centered cubic, BCC: body centered cubic and HCP: hexagonal close packed)

The temperature was increased to 3000 K within 10 ps, held at this temperature for 10 ps, and cooled within 10 p by reducing the temperature to 300 K ( $\sim 10^{14}$  K/s) to investigate the phase transformation mechanism of the Fe-Cr-Ni system from the liquid to the solid phase. Figure 7 shows the total RDF curves obtained at 3000 K and 300 K during the cooling process. When the RDF curves were analyzed at 3000 K, the structure completely melted, representing the liquid phase. As a result of the rapid cooling at 300 K, the transformation of the structure into an amorphous type or glassy structure was realized. The splitting in the second peak of the RDF curve is characteristic of glassy structures and indicates the presence of atomic correlation in the second neighborhood compared to the liquid phase [27]. At the final of the cooling process, the fractions of the most dominant crystal lattices of FCC, BCC, HCP, icosahedral (ICO), and other structures in the MD cell were calculated as 0.3, 0.4, 1.1, 0.9, and 97.3 percent at 300 K, respectively. These results indicated that the formation of ICO/HCP forms a significant fraction in the glass Fe-Cr-Ni alloy.

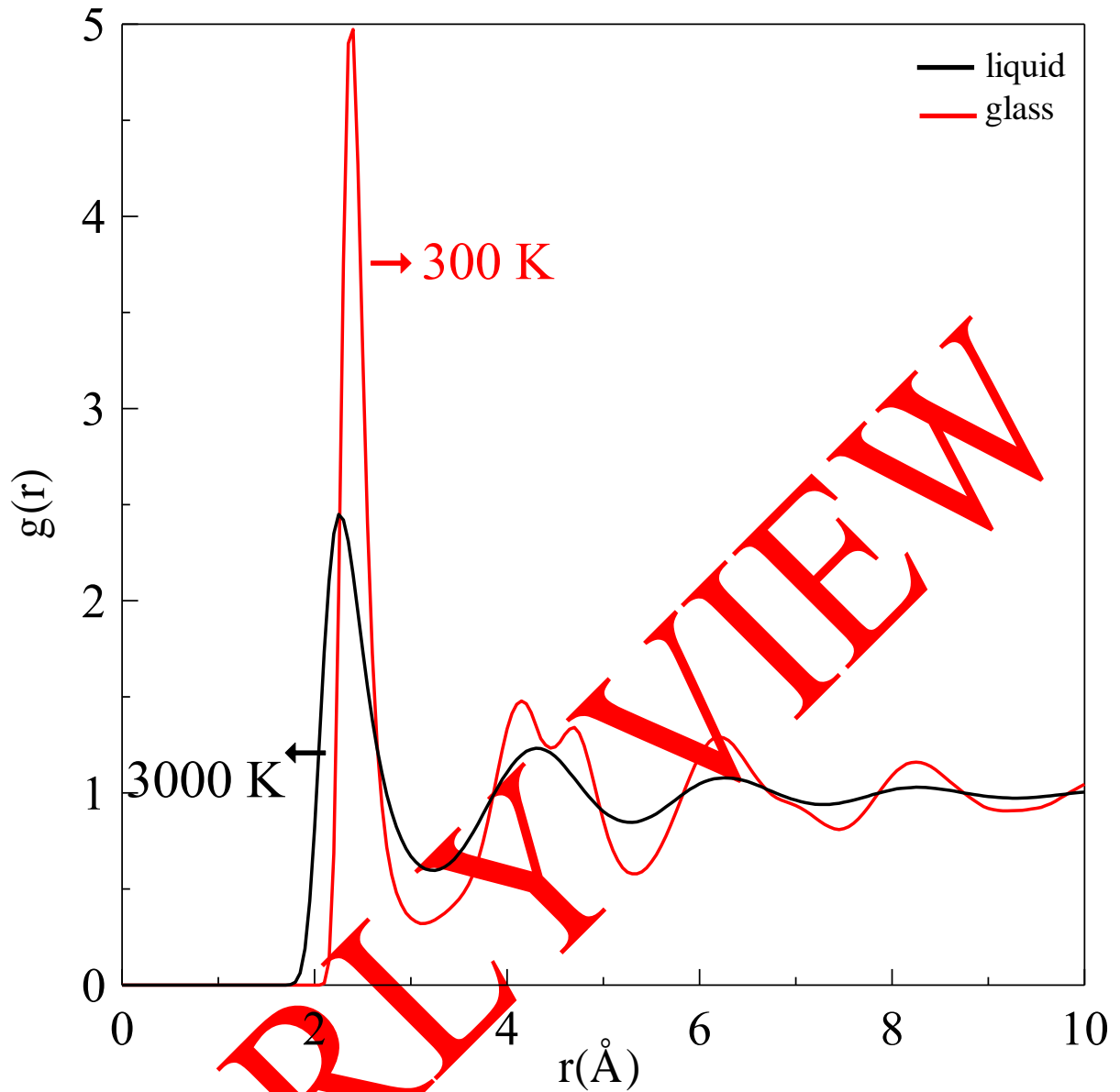


**Figure 7.** The RDF curves obtained at 300 K and 3000 K temperatures during the rapid cooling process of the model system

#### 4. RESULTS

In this study, Fe-Cr-Ni ternary alloy system was modelled by molecular dynamics (MD) method based on Gruzicic-Zhou (GZ) type potential energy function. The model system was subjected to different heat treatments and the phase transformation mechanisms in these processes were investigated with different analysis methods. The results obtained were compared with the experimental data and it was seen that the results were compatible with the experimental data.

For the model system, it is seen that the FCC ( $\gamma$ ) phase does not change between the temperature of 1000-1100 K and in the region of high concentration (as atomic percentage) of Ni atoms and low concentrations of Fe and Cr atoms during the heating process. The Fe-Cr-Ni system, which was kept for 10 ps at 3000 K, was stabilized at 300 K using high cooling rate and it was determined that the system turned into glass (amorphous) phase.

In the future studies, the concentration ratios of Cr, Fe and Ni elements, which form the binary and ternary systems, are selected for a single region of the phase diagram. Studies can be repeated according to different concentration ratios and the results can be compared using different potential functions for model system.

### CONFLICTS OF INTEREST

No conflict of interest was declared by the authors.

### REFERENCES

- [1] Wang, J., Han, W. Q., “A review of heteroatom doped materials for advanced lithium–sulfur batteries”, *Advanced Functional Materials*, 32(2): 2107166, (2022).
- [2] Chen, K., Ma, Z., Li, X., Kang, J., Ma, D., Chu, K., “Single-Atom Bi Alloyed Pd Metallene for Nitrate Electroreduction to Ammonia”, *Advanced Functional Materials*, 33: 2209890, (2023).
- [3] Shi, M., Wang, R., Li, L., Chen, N., Xiao, P., Yan, C., Yan, X., “Redox-active polymer integrated with MXene for ultra-stable and fast aqueous proton storage”, *Advanced Functional Materials*, 33(1): 2209777, (2023).
- [4] George, E. P., Raabe, D., Ritchie, R. O., “High-entropy alloys”, *Nature Reviews Materials*, 4(8): 515-534, (2019).
- [5] Miracle, D. B., Senkov, O. N., “A critical review of high entropy alloys and related concepts”, *Acta Materialia*, 122, 448-511, (2017).
- [6] Wang, J., Jiang, P., Yuan, F., Wu, X., “Chemical medium-range order in a medium-entropy alloy”, *Nature Communications*, 13(1): 1021, (2022).
- [7] Yang, G., Kang, J., Carsbring, A., Mu, W., Hedström, P., Kim, J. K., Park, J. H., “Heterogeneous grain size and enhanced hardness by precipitation of the BCC particles in medium entropy Fe–Ni–Cr alloys”, *Journal of Alloys and Compounds*, 931: 167580, (2023).
- [8] Nguyen, T. D., Zhang, J., Young, D. J., “Effects of silicon on high temperature corrosion of Fe–Cr and Fe–Cr–Ni alloys in carbon dioxide”, *Oxidation of Metals*, 81: 549-574, (2014).
- [9] Miettinen, J., “Thermodynamic reassessment of Fe-Cr-Ni system with emphasis on the iron-rich corner”, *Calphad*, 23(2): 231-248, (1999).
- [10] Du, X., Ma, X., Ding, X., Zhang, W., He, Y., “Enhanced high-temperature oxidation resistance of low-cost Fe–Cr–Ni medium entropy alloy by Ce-adulterated”, *Journal of Materials Research and Technology*, 16:1466-1477, (2022).
- [11] Blinova, E. N., Glezer, A. M., Libman, M. A., & Pimenov, E. V., “Influence of Severe Plastic Deformations on Martensitic Transformation in Alloys of Fe-Cr-Ni System”, *In Key Engineering Materials*, 910:802-807, (2022).
- [12] Mahesh, B. V., Raman, R. S., Koch, C. C., “Bimodal grain size distribution: an effective approach for improving the mechanical and corrosion properties of Fe–Cr–Ni alloys”, *Journal of Materials Science*, 47:7735-7743, (2012).
- [13] Du, X., Ma, X., Ding, X., Zhang, W., He, Y., “Enhanced high-temperature oxidation resistance of low-cost Fe–Cr–Ni medium entropy alloy by Ce-adulterated”, *Journal of Materials Research and Technology*, 16: 1466-1477, (2022).

- [14] Zhang, C., Wang, C., Zhang, S. L., Ding, Y. L., Ge, Q. L., Su, J., “Effect of aging temperature on the precipitation behavior and mechanical properties of Fe–Cr–Ni maraging stainless steel”, *Materials Science and Engineering: A*, 806: 140763, (2021).
- [15] Biskri, Z. E., Rached, H., Boucheur, M., Rached, D., “Computational study of structural, elastic and electronic properties of lithium disilicate ( $\text{Li}_2\text{Si}_2\text{O}_5$ ) glass-ceramic”, *Journal of the Mechanical Behavior of Biomedical Materials*, 32: 345-350, (2014).
- [16] Sengul, S., Celtek, M., Domekeli, U., “Molecular dynamics simulations of glass formation and atomic structures in  $\text{Zr}_{60}\text{Cu}_{20}\text{Fe}_{20}$  ternary bulk metallic alloy”, *Vacuum*, 136:20-27, (2017).
- [17] Ozgen, S., Duruk, E., “Molecular dynamics simulation of solidification kinetics of aluminium using Sutton–Chen version of EAM”, *Materials Letters*, 58(6):1071-1075, (2004).
- [18] Celik, F. A., Yildiz, A. K., Ozgen, S., “A molecular dynamics study to investigate the local atomic arrangements during martensitic phase transformations”, *Molecular Simulation*, 37(05):421-429, (2011).
- [19] Celtek, M., “Atomic structure of  $\text{Cu}_{60}\text{Ti}_{20}\text{Zr}_{20}$  metallic glass under high pressures”, *Intermetallics*, 143:107493, (2022).
- [20] Mahata, A. K., Kivy, M. B. “Computational study of nanoscale mechanical properties of Fe–Cr–Ni alloy”, *Molecular Simulation*, 48(7): 551-567, (2022).
- [21] Wu, C., Lee, B. J., Su, X., “Modified embedded-atom interatomic potential for Fe-Ni, Cr-Ni and Fe-Cr-Ni systems”, *Calphad*, 57:98-106, (2017).
- [22] You, L. J., Hu, L. J., Xie, Y. P., Zhao, S. J., “Influence of Cu precipitation on tensile properties of Fe–Cu–Ni ternary alloy at different temperatures by molecular dynamics simulation”, *Computational Materials Science*, 118: 236-244, (2016).
- [23] Das, N. K., Suzuki, K., Ogawa, K., Shoji, T., “Early stage SCC initiation analysis of fcc Fe–Cr–Ni ternary alloy at 288 °C: A quantum chemical molecular dynamics approach”, *Corrosion Science*, 51(4): 908-913, (2009).
- [24] Wang, L., Kamachali, R. D., “Density-based grain boundary phase diagrams: Application to Fe-Mn-Cr, Fe-Mn-Ni, Fe-Mn-Co, Fe-Cr-Ni and Fe-Cr-Co alloy systems”, *Acta Materialia*, 207: 116668, (2021).
- [25] Kumar, S., Nandi, S., Pattanayek, S. K., Madan, M., Kaushik, B., Kumar, R., Krishna, K. G., “Atomistic characterization of multi nano-crystal formation process in Fe–Cr–Ni alloy during directional solidification: Perspective to the additive manufacturing”, *Materials Chemistry and Physics*, 308: 128242, (2023).
- [26] Daw, M. S., Foiles, S. M., Baskes, M. I., “The embedded-atom method: a review of theory and applications”, *Materials Science Reports*, 9(7-8): 251-310, (1993).
- [27] Smith, R. W., Was, G. S., “Application of molecular dynamics to the study of hydrogen embrittlement in Ni-Cr-Fe alloys”, *Physical Review B*, 40(15): 10322, (1989).
- [28] Fujitsu Limited., 2021, Tokyo, Japan, ([www.sicgress.com](http://www.sicgress.com)).
- [29] Hoover, W. G., “Canonical dynamics: Equilibrium phase-space distributions”, *Physical Review A*, 31(3):1695, (1985).
- [30] Tanaka, H., “Relationship among glass-forming ability, fragility, and short-range bond ordering of liquids”, *Journal of Non-Crystalline Solids*, 351(8-9): 678-690, (2005).

- [31] Raghavan, V., “Cr-Fe-Ni (chromium-iron-nickel)”, *Journal of Phase Equilibria and Diffusion*, 30(1): 94-95, (2009).
- [32] Trady, S., Mazroui, M., Hasnaoui, A., Saadouni, K., “Molecular dynamics study of atomic-level structure in monatomic metallic glass”, *Journal of Non-Crystalline Solids*, 443: 136-142, (2016).
- [33] Pei, Q. X., Lu, C., Lee, H. P., “Crystallization of amorphous alloy during isothermal annealing: a molecular dynamics study”, *Journal of Physics: Condensed Matter*, 17(10):1493, (2005).
- [34] Stukowski, A., “Visualization and analysis of atomistic simulation data with OVITO—the Open Visualization Tool”, *Modelling and Simulation in Materials Science and Engineering*, 18(1): 015012, (2009).

**EARLY VIEW**